

Cranfield University

Richard Smith

Improving fatigue performance of steel
T-joint welds – a pilot study

School of Applied Sciences

Welding Engineering

M.Sc.

2011

S. Williams, D. Yapp

05 Sept 2011

This Thesis is submitted in partial fulfilment of the Degree of Master of Science

© Cranfield University, 2011. All rights reserved. No part of this publication may be reproduced without written permission of the copyright holder

Abstract

Welds tend to have low fatigue performance, limiting the design stress of the structure to low levels whenever the loading is dynamic. Metal fatigue affects ships, bridges, cranes and earthmoving equipment as the service loading is cyclic - example for ships is wave action.

This pilot study sought fatigue life improvement for these applications. Laser welding is now readily available and Hybrid Laser Arc Welding (HLAW) offered promise. HLAW's were compared to conventional GMAW (MIG) and FCW T-fillet welds. Alternate-side HLAW's used keyhole-mode laser welding with GMAW to get full-penetration T-butt joints which performed well in fatigue test; never less than 1.5 times the endurance predicted for fillet welds in BS7608 and EN1993 standards. Small profile-bead size attainable for HLAW's simplified TIG-dressing, implying HLAW+TIG-dress might be economically viable. HLAW+TIG-dress welds could not be fatigued for these transverse non-load-bearing T-joints loaded in uniaxial pulsating tension, one sample surviving 2.3million cycles at 0.6 of the nominal yield stress of the 355MPa plate steel. Magnetic-particle inspection indicated no cracks, implying a fatigue crack initiation phase dominates fatigue endurance of these HLAW+TIG-dress samples which would fail in about 250thousand cycles of crack growth phase after crack initiation had occurred.

The HLAW's as-welded perform well and are very economic, with welding speed 2 to 4 times faster than GMAW/FCW fillet-welds. HLAW+TIG-dress fatigue performance is so high it suggests looking to designs using 490MPa steel in fully dynamic loading.

Acknowledgments

I would like to make these thanks to members of Cranfield University:

Professor Stewart Williams and Mr David Yapp who respectively brought the ship-construction and the earthmoving machinery, cranes and bridges parts of the project to the WERC, then supervised this project which I found so interesting.

The WERC's technicians: Mr Flemming Neilsen, always helpful and Mr Brian Brookes, providing a wealth of accumulated knowledge.

Mr Wojciech Suder, PhD student at the WERC, whose ability to “drive” the laser-welding equipment enabled desired welds to be quickly obtained

Dr Paul Colegrove, Course Director of the Welding Engineering course, whose gift for concepts and mathematical representation he was always willing to share.

Dr Isidro Durazo-Cardenas, manager of the fatigue-testing laboratory who coped with my campaign of fatigue-testing and Mr Andy Dyer, metallography laboratory manager, who accommodated my metallographic needs.

My colleagues who had time for cheer while labouring at their projects.

Further afield thanks go to:

Mr John Jubb, retired former lecturer of Cranfield University and contributor in the world of fatigue especially in marine applications, who was giving of his time and ever-helpful as I made my way through the learning journey into the subject of metal-fatigue.

My ever-tolerant and supportive lady-friend.

Finally I must round-off by giving unspecified credit to all those who provided helpful comment, information, advice and encouragement

Contents

1	Review of literature	2
1.1	Weld performance	2
1.1.1	Arc characteristics of wire-fed processes	2
1.1.2	Weld residual stresses	2
1.1.3	Hybrid Laser Arc Welding (HLAW)	3
1.2	Fatigue performance	3
1.2.1	Conventional welds show low fatigue endurance	3
1.2.2	Weld fatigue endurance not function of mean stress	4
1.2.3	Weld dressing	4
2	Method	6
2.1	Design of experimental programme	6
2.2	The project stages	6
2.3	Methods applying selected conditions	7
2.3.1	Welding to create representative samples	7
2.3.2	Fatigue testing	9
2.4	Methods investigating the test outcome	10
2.4.1	Welding machine output through data-logging	10
2.4.2	Magnetic particle inspection	11
2.4.3	Metallography	11
2.5	Welding conditions for fatigue samples	12
2.5.1	Conventional GMAW and 5mm S355 plate	12
2.5.2	Conventional FCAW and 6mm DH36 plate	12
2.5.3	HLAW and 6mm DH36 plate weld development	12
2.5.4	HLAW and 6mm DH36 plate for fatigue testing	13
2.5.5	TIG-dressing of HLAW on 6mm plate	13
3	Results	15
3.1	Current-practice MIG and FCAW T-fillet welds	15
3.2	Hybrid Laser-Arc Welds (HLAW's)	15
3.2.1	HLAW samples for fatigue testing	19

3.2.2	TIG-dressing of hybrid laser/MIG welds	21
3.3	Fatigue testing of the weld samples	21
3.3.1	Fatigue endurance	21
3.3.2	General appearance of fatigue breaks	24
4	Discussion	27
4.1	The welding conditions development	27
4.1.1	Current-practice MIG and FCAW T-fillet welds	27
4.1.2	Hybrid Laser-Arc Welds (HLAW's)	27
4.2	Hybrid Laser/MIG weld surface remelt dressing treatments	29
4.2.1	The TIG dressing technique	29
4.2.2	TIG-dressing performance	30
4.2.3	TIG-dressing in a commercially viable welding option	30
4.3	The fatigue testing programme	31
4.3.1	Use of non-load-bearing T-joint tests	31
4.3.2	The 0.6 of Yield Stress fatigue test condition	31
4.3.3	Conventional MIG and FCAW cycled to the nominal yield stress	32
4.3.4	Conventional MIG and FCAW in S-N range	33
4.3.5	HLAW as-welded fatigue tests	34
4.3.6	HLAW+TIG-dressed weld fatigue tests	35
5	Conclusions	36
	Bibliography	38

List of Figures

2.1	Non-Load-Bearing (NLB) T-joint sample	7
2.2	Conventional welding equipment for GMAW and FCAW of T-joint samples.	8
2.3	HLAW set-up, for hybrid laser with GMAW	8
2.4	Fatigue-testing machine; a uniaxial load servo-hydraulic machine	9
2.5	Stress-cycles for R=0 and R=0.1 when S_r is unity	10
2.6	The MPI technique for investigating presence of fatigue cracks	11
2.7	Conditions used for TIG-dressing: LHS - single-run; RHS - two runs or two torches	13
3.1	Weld surfaces of FCAW's	16
3.2	V-I plots of FCAW and GMAW datalogs	16
3.3	HLAW's at different laser powers - by row from top: 3.0kW, 3.5kW, 4.0kW and 4.5kW	17
3.4	HLAW microstructures for 4.5kW - centre, HAZ and fusion-root	18
3.5	Cleanness and soundness of HLAW with 4.5kW laser beam power	19
3.6	HLAW as-welded surfaces	20
3.7	HLAW and laser weld with shrinkage cracks	20
3.8	Arc waveforms: LHS - HLAW; RHS - manual "RapidArc" weld	20
3.9	TIG-dressed HLAW using the single-run technique	21
3.10	TIG-dressed HLAW using the two-run technique: overall ap- pearance and two sections at different locations	22
3.11	S-N curve presentation of fatigue-endurance data	24
3.12	Sample endurance in ratio to the BS7608:1993 "Class F" mean endurance	25
3.13	Fractured fatigue sample	25
3.14	Early-stage fatigue crack, seen at top of image	26
4.1	Toe-groove or "undercut": the unequal consequences of erring about the ideal condition	33

List of Tables

- 3.1 Fatigue endurance observations for the T-joint weld samples . 23

Notations

LHS Left Hand Side

RHS Right Hand Side

HLAW Hybrid Laser-Arc Welding (“arc” signifying any electric-arc process
- MIG, TIG, *etc*)

MIG Metal Inert Gas [welding] (synonym of GMAW)

GMAW Gas Metal Arc Welding (synonym of MIG)

FCAW Flux Cored Arc Welding

TIG Tungsten Inert Gas [welding] (synonym of GTAW)

GTAW Gas Tungsten Arc Welding (synonym of TIG)

CV Constant Voltage (applying to an arc-welding process)

WERC Welding Engineering Research Centre of Cranfield University

σ stress

σ_y yield stress of a metal

σ_{\min} minimum stress

σ_{\max} maximum stress

S stress-range in a fatigue-test, between σ_{\min} and σ_{\max}

S_r synonymous with S ; the stress-range

N number of fatigue cycles to failure

N_{mean} expected mean number of fatigue cycles to failure

Introduction

A call to reconsider what is now possible with welding came from two sources simultaneously. Improved fatigue-resisting performance for welds received early mention, given how design-limiting this issue tends to be. Lasers have become cheaper, robust, easy to use and more powerful. The instinctive question is whether lasers in welding might provide new opportunities for higher-performance welds, since the last time the issue was visited. Then welding reconsidered might identify other new technologies useful to structural welding.

Shipbuilding produced a call for better ships. For certain a better ship is

- cheaper
- faster
- consumes less fuel
- carries more cargo / payload
- requires less maintenance

Seagoing ships suffer cyclic loading throughout their lives by sailing through waves, making improved fatigue performance a primarily desirable characteristic. Approximately 80% of shipbuilding for passenger and military ships are lighter rib-stiffened flat panels for the decks and interior compartments, with plate thicknesses in millimetres. Improving fatigue resistance of the many T-joints of stiffer-to-plate would be very beneficial. Cargo ships have a profusion of stiffeners on greater plate thickness bulkheads and outer hull-form structures whose T-joints may benefit from new methods identified.

The other call came simultaneously from a consortium representing land-based applications where fatigue is a pressing issue: for earthmoving equipment, cranes and bridges. These use many T-joints sharing similarities with those in marine structures - particularly the dynamic-load duty where metal fatigue avoidance is usually the limiting design factor.

The necessary project to define answers would be extensive. This study embarked as a pilot-study, seeking advantageous possibilities and estimating how advantageous these might be.

Chapter 1

Review of literature

1.1 Weld performance

1.1.1 Arc characteristics of wire-fed processes

GMAW can be operated in different transfer-modes [1]. Low energies give dip transfer [1], a cyclical mode of alternate arcing and dipping of the filler wire into the weldpool. At currents and voltages just high enough to cease dipping there is globular transfer. With further increase in current, transition from occasional transfer of large spheres of metal of globular-transfer to the forceful spray transfer delivering a stream of fine droplets is shown to be at a tipping point where magnetic pinch pressure due to current overcomes surface tension [2]. The transition from globular transfer to spray transfer is shown to occur over a brief interval of changing current [2].

1.1.2 Weld residual stresses

The thermal cycle of welds leaves a static state of unchanging high residual stress in a weldment on completion of the weld [3]. The central region of a weld which is at the yield stress of the material [3, 4, 5]

The tendency to buckling is shown to be an almost linear relationship between weld heat input and severity of distortion [3]. It was also shown [3] that for their 4mm plate thickness the threshold heat input below which the critical buckling load would not be exceeded was very low; beneath that of any arc process and only achievable in an autogenous laser weld. However the laser-only weld had defective shape, with undercut.

HLAW had lower heat input and therefore less buckling distortion than any arc-only welding process [3], though both were higher than for the laser-only weld.

A finding that for given weld penetration depth, yield-stress-level residual stress domain in HLAW's is 50% larger than in a laser (only) weld [6] concurs.

Residual stresses affect the fatigue endurance characteristics of welds, Section 1.2.2.

1.1.3 Hybrid Laser Arc Welding (HLAW)

The intention is to get the deep penetration of a laser weld so that the weld is completed in one pass, combined with the forgiving nature of an arc weld which can cope with variable joint set-up (within reasonable limits) [7].

An extensive investigation [8] identified that the ideal axis-to-axis distance of laser and arc as they are incident on the plate surface would be closer than their minimum of 4.5mm.

Investigation over a range from no separation - the arc and laser apply themselves to the weldment at the same location - to 7mm axis-to-axis separation found the ideal axis-to-axis separation is 2mm, giving deepest weld penetration [9]. No separation gives an unstable welding condition, manifestations including weld pool turbulence. It is conjectured that molten metal droplets intermittently landing on the "keyhole" formed in the weldpool by the laser-beam is the cause of that instability.

An etched cross-section of a co-planar butt weld has a depth to width of 1.5 and in all other ways the weld looks very satisfactory. There is uniform taper, narrowing from widest at the plate surface the narrow at the fusion root.

Both investigators [8, 9] had the laser-beam leading the arc ("laser leading").

1.2 Fatigue performance

1.2.1 Conventional welds show low fatigue endurance

In the general case of "non-welds", such as engineering components machined from wrought bar-stock, fatigue strength increases as yield strength increases [10].

The observation that fatigue strength of welds is independent of the strength of the plate being welded was puzzling. Even more so that heat-treatment of the weldment did not change the effect - which ruled out heat-affect-zone (HAZ) microstructure as an explanation [10].

A major contribution was made in 1967 with an analysis and investigation [10] of the subject. Metallography of the weld toe region where fa-

tigue cracks initiated, on cross-sections and at increasing depths parallel to the prior plate surface, showed many slag defects at the weld toe. This is the region which has been molten or pasty at the peripheral region of the weld, just inside the weld. On high-magnification inspection very sharp-tipped slag-filled defects were observed, estimated to have tip radius less than 1.3×10^{-5} m. Machining notches with this tip radius into various steels of different strengths produced an interesting result: they all gave the same fatigue endurance. They mathematically showed that defect depth of 0.4mm, which they saw, would be expected to be critical and propagate at $S_r = 108$ MPa in the stress-concentration at the weld-toe of a fillet-weld. The point is made that smaller defect size places them more inside the highest geometric stress concentration factor of the general shape of the toe region of weld-to-plate. “Weld toe intrusions” remains the accepted explanation why traditional welds have fatigue strength independent of material strength.

1.2.2 Weld fatigue endurance not function of mean stress

Yield-stress-level residual stresses cause fatigue endurance of welds to show no dependence on the mean stress; only on the stress range [4, 5]. This is reflected in fatigue design Standards [11, 12]; they relate fatigue life only to stress-range S , except allowance for post-weld stress relieve heat treatment in special cases [12].

1.2.3 Weld dressing

The finding that weld toe intrusions - sharp-tipped small slag-filled defects just inside the edge of the weld metal - caused a substantial loss of fatigue performance for welds [10] logically lead to the concept of dressing the weld toe in some way which removes or contains the effects of those defects. Grinding the toe had already been tried [10], which was reported as restoring a relationship between the strength of the steel and the fatigue endurance. Peening the weld surface is also mentioned [10].

There have followed some large-scale investigations on weld-toe dressing for improving weld fatigue endurance by The Welding Institute in the UK [13, 14] and the International Institute of Welding [15].

Two families of approaches are categorised [13]. “Modification of weld toe geometry” is where the the weld toe intrusions are removed and the shape transitioning between weld-metal and plate is smoothed. This category includes weld toe-grinding and remelt-dressing. “Modification of residual stress

distribution” change the weld residual stresses in the vulnerable weld toe region in a beneficial way; relaxing it or even changing it into a residual compressive stress. This approach includes post-weld heat-treatment (PWHT) stress-relief, weld peening and spot-heating in controlled ways near the weld.

Testing of the dressed welds included fatigue testing at constant stress amplitude and fatigue testing under variable amplitude loading simulating wave action on oil-rigs [13].

For weld toe-grinding, fatigue failure remains generally at the weld toe, while fatigue endurance increased 5-fold for medium-strength steels and 6-fold for high-strength steels.

For TIG-dressed welds half the samples failed in fatigue at locations other than the weld toe. This implies the weld has become very fatigue-resistant, evidently on par with the hot-rolled plate steel it is welding. It was accepted that the TIG-dressed welds attained the fatigue resistance of a hot-rolled section. TIG-dressed joints were shown to retain their advantage under all loadings which could be devised.

For toe-ground welds an increase in fatigue design life of 2.2 was found to be justified [14], compared to as-welded fillet welds. They found fatigue cracks initiating in the ground weld toe from around 20% of the fatigue life the samples ultimately achieved. This indicates that creating an extensive crack initiation stage is not the explanation for the fatigue endurance improvement of toe-grinding. They conclude that the improvement from toe-grinding is from lowering the stress intensity factor in the weld toe region from smoothing the geometric shape; from changing cracks growing to a less harmful shape which propagates less rapidly and possibly from the ground depth of the groove being in a lower residual stress region compared to the surrounding plate surface.

The large survey into weld dressing [15] is focused on good Trade technique for applying weld dressing; hence is outside academic interest.

Chapter 2

Method

2.1 Design of experimental programme

The engineering application of interest is the performance of welded T-joints. Hence, the experimental programme was centred on sample T-joint welds.

The fatigue properties of welds produced is the primary interest. Two considerations indicate which fatigue test sample configuration to select:

- In the engineering application, the main loads on the structure are in the plane of the plate.
- when fatigue loadings are equal in all directions in the plane of the plate, welds are more vulnerable to the transverse fatigue loading than the longitudinal fatigue loading [4, 5, 11, 12]

It follows that the appropriate fatigue test configuration is the axially-loaded plate sample with transverse non-load-bearing (NLB) weld (also referred to in literature as transverse non-load-carrying welds *eg* [4]).

A NLB T-joint sample is shown in 2.1.

2.2 The project stages

An initial phase used a stock of commonly-available commercial materials to trial the techniques and experience the “learning curve” associated with them. Results obtained are of value and form part of the outcome. Standard structural steel plate, 5mm thick BS EN 10025 “S355” [16] was MIG welded and hybrid laser/MIG welded (a specific variant of HLAW). All MIG wire was specification ISO 14341-A : G 46 4 M G4Si1 [17].

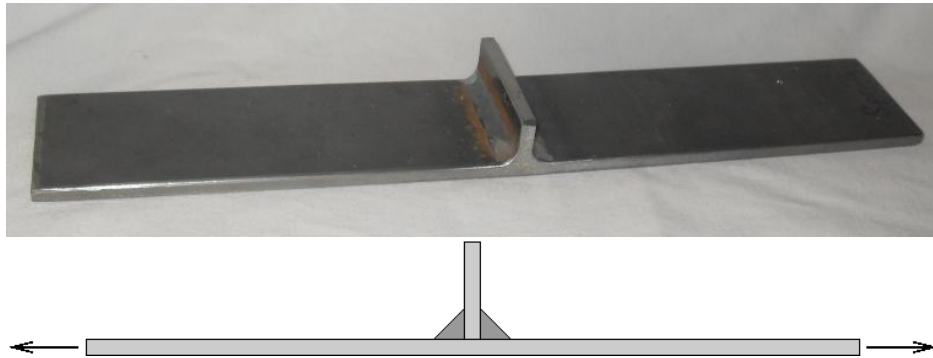


Figure 2.1: Non-Load-Bearing (NLB) T-joint sample

Shielding gas of stated composition $\text{Ar}20\%\text{CO}_2\ 2\%\text{O}_2$, specification ISO 14175 M26 [18] was used at a flow rate of 18litres per minute for all welds in this study.

The second stage applied these techniques to specifically shipbuilding materials. Steel was of American Bureau of Shipping 355MPa yield strength specification “DH36” [19]. Contemporary specification fillet welds were welded with Rutile flux-cored-wire of specification ISO 17632-A: T 42 2 Z P M 1 H5 [20]. HLAW’s used the same MIG wire of ISO 14341-A : G 46 4 M G4Si1 specification as for the initial phase.

Steels S355 and DH36 are sufficiently similar that findings for one steel are likely to apply to both.

2.3 Methods applying selected conditions

2.3.1 Welding to create representative samples

All welding of the representative samples tested was mechanised welding. All laser welding was performed in “keyhole mode” [21].

Conventional GMAW (MIG) and FCAW was performed using a high-specification commercially available GMAW machine applying itself through a mechanised-welding torch mounted on a 3-axis Cartesian manipulator. A general view of the torch and sample set-up is shown, Figure 2.2. To the LHS is the Cartesian 3-axis manipulator and torch at 45° tilt; to RHS the welding machine (red).

A manual welding torch was sometimes coupled to this welding machine to facilitate exploring welding conditions rapidly and for producing physically “model” weld runs in dip-transfer, spray-transfer and pulsed-transfer modes when familiarising with the data-logging.



Figure 2.2: Conventional welding equipment for GMAW and FCAW of T-joint samples.



Figure 2.3: HLAW set-up, for hybrid laser with GMAW

Hybrid GMAW/laser welding was performed in a facility dedicated to laser welding, as necessitated by the safety issues of using a laser beam. Enforceable exclusion of operators and any other persons when the beam is activated is required. A view of the torch and laser beam delivery optic is presented in Figure 2.3. To the LHS is laser beam delivery optic; to the RHS is the MIG torch. The jig holding the sample is similar to jig for conventional welding of Fig 2.2. The GMAW machine was the same model as that used for conventional GMAW. The laser is a commercial “YLR-8000” 8kW fibre laser by IPG Photonics, remote from the welding activity delivering through a fibre-optic to the beam delivery optic seen in Figure 2.3.



Figure 2.4: Fatigue-testing machine; a uniaxial load servo-hydraulic machine

2.3.2 Fatigue testing

The fatigue testing machine

A 250kN maximum load servo-hydraulic axial fatigue testing machine was used for all fatigue tests. This testing machine is able to apply the dynamic loading specified at 10Hz for all loads used. Thus, a 2×10^6 cycle test takes 56hours. The machine with typical test (5mm S355; first sample of 110602) is shown in Figure 2.4. The LHS image shows the testing machine. The RHS image is a close-up of the grips holding a fatigue sample

Fatigue test samples - obtaining, dimensions, preparation

The form of the sample was presented in Figure 2.1 on page 7.

Fatigue test samples were sawn from the test welds by transverse cuts across the width of the weld sample.

The width of the fatigue sample is $10 \times$ the sample thickness. *Eg* a sample from 6mm plate is 60mm wide. No guidance on this issue was identified. The decision basis is a sample which balances moderate test loads (smaller width) against preserving some characteristics of a long weld (larger width).

Engineering application behaviour is best represented by fatigue crack initiation along the mid-length of the weld. To predispose this behaviour by eliminating extraneous crack initiation sites, the sample edge surfaces and corners were smoothed by filing and/or grinding then finishing and rubbing with abrasive-paper. The abrupt sharp-featured termination of the sampled weld at the sawn edges were treated in this way.

The fatigue cycle applied

All tests applied a pulsating-tension load-cycle in the form of a sine-wave.

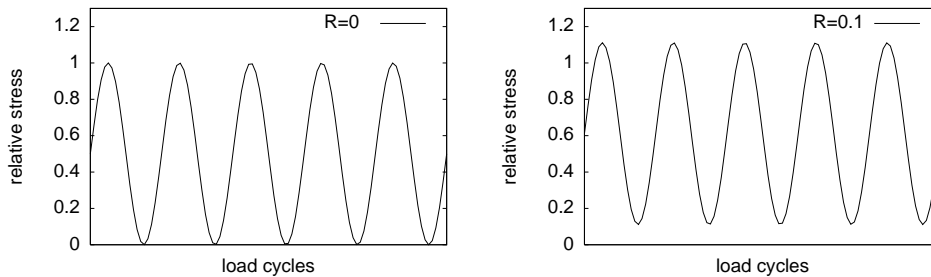


Figure 2.5: Stress-cycles for $R=0$ and $R=0.1$ when S_r is unity

An “R-value” of 0.1 was used as the best way to define like-for-like tests at different loads. This avoids the practical problem of mechanical “clanking” the fatigue testing machine suffers if the load goes to zero on each cycle for an “R-value” of 0 which would otherwise be preferred. The issue is explained graphically for the same stress range of unity but where $R=0$ and $R=0.1$ in Figure 2.5.

Guidance for testing conditions

The easy-to-apply but largely superseded BS7608:1993 [11] was used to estimate expected fatigue lives in specifying test conditions. The “mean life” relationship [11, (Fig. 8 pg41)] is used to identify suitable S_r vs N_{mean} combinations when aiming along a spectrum between high-stress low-endurance tests and low-stress high-endurance tests.

Conventional fillet welds are widely help to have fatigue endurances conforming to BS7608:1993 Class F [11, (Type number 5.2 pg12)].

2.4 Methods investigating the test outcome

2.4.1 Welding machine output through data-logging

A Triton Electronics “AMV4000” welding-monitor was used to measure and record the welding current, voltage and wire-feed-speed (WFS) at a given sampling rate, typically several thousand logs per second (Hz).

The log obtained from the weld monitor as a text-file was post-processed with the standard familiar “unix toolkit” to true average arc-power - the average of the instantaneous $V \times I$ products - and graphical representation of arc V vs I characteristics.



Figure 2.6: The MPI technique for investigating presence of fatigue cracks

2.4.2 Magnetic particle inspection

The magnetic particle inspection (MPI) technique applied is shown in Figure 2.6.

The technique was used to investigate whether fatigue cracks had already formed in sample which had been fatigued but were as-yet unbroken.

The samples were magnetised by a “horseshoe” shaped permanent magnet demonstrated to be able lift a steel 20kg steel object. Applied to the underside of the sample, the pole gap straddles the location of the T-joint. A thin layer of a white primer paint was used in lieu of “contrast paint” of formal MPI procedures. A spray-applied paraffin-based system of black magnetic particles was kept mobile by additional “white spirit” (medium petroleum distillate) where particles were not strongly bound to sample defects.

2.4.3 Metallography

Standard metallographical laboratory techniques were used to examine sections across samples on macroscopic and microscopic scales. Samples were etched or unetched depending on features being examined.

The sample face of interest was ground through successively finer abrasive grits, using standard abrasive papers. Macro-etching was performed with 10% Nital (nitric acid in methanol). Micro-polishing used $0.25\mu\text{m}$ silica suspension in a cloth polishing-wheel. Micro-etching used 2% Nital (Nitric acid in alcohol).

2.5 Welding conditions for fatigue samples

2.5.1 Conventional GMAW and 5mm S355 plate

Conventional MIG welding provided fatigue-test samples welded in dip-transfer mode and welded in spray-transfer mode, with these conditions:

Sample id	WFS (m/min)	Current (A)	Volts (V)	Arc power (kW)	Weld TS (m/min)	Arc energy (kJ/mm)
Dip-MIG	5.59	216.3	22.1	4.78	0.42	0.68
Spray-MIG	6.22	241.1	28.2	6.80	0.42	0.97

2.5.2 Conventional FCAW and 6mm DH36 plate

Two FCAW's later fatigue-tested were welded with conditions:

Sample id	WFS (m/min)	Current (A)	Volts (V)	Arc power (kW)	Weld TS (m/min)	Arc energy (kJ/mm)
305/23.0	7.75	225	23.0	5.18	0.5	0.62
320/23.5	8.13	236	23.5	5.55	0.5	0.67

2.5.3 HLAW and 6mm DH36 plate weld development

These welds sought to penetrate more than half-way through the weld joint thickness without being full-penetration. Thus, a joint welded on alternate sides by the same welding activity would be full-penetration joint.

The necessary laser power to ensure fusion beyond the mid-thickness of the terminating "T" plate, such that alternate-side welding would give a full-penetration joint, was investigated.

These welding conditions were not varied:

leading - arc or laser	arc
axis-to-axis laser/arc(mm)	2.0
weld TS (m/min)	1.0
arc WFS (m/min)	4.0
arc "trim"	1.00
arc power (kW)	3.0
arc energy (kJ/mm)	0.18
laser-beam diameter (mm)	0.95

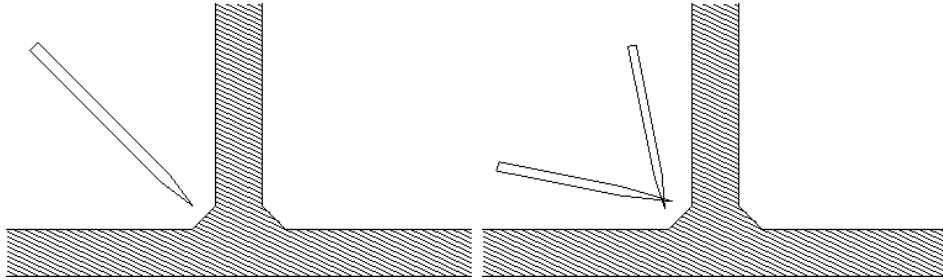


Figure 2.7: Conditions used for TIG-dressing: LHS - single-run; RHS - two runs or two torches

Arc-torch slope and tilt were 66° giving drag angle and 45° , respectively; laser slope and tilt were 90° and 15° respectively.

Laser beam powers of 3.0kW, 3.5kW, 4.0kW and 4.5kW were tried during HLAW.

2.5.4 HLAW and 6mm DH36 plate for fatigue testing

All these welds were alternate-side welded with identical welding conditions for the two sides of any one T-joint.

Two welding conditions were used:

- The 4.5kW laser-beam power condition of the previous Section 2.5.3
- Travel-speed (TS) doubled to 2m/min; wire-feed-speed (WFS) doubled to 8m/min giving arc power of 5.7kW. Retaining the same WFS/TS ratio would, all other things being equal, give the same deposition of weld-metal. Laser power was increased to 5.5kW.

2.5.5 TIG-dressing of HLAW on 6mm plate

Only 6mm thickness DH36 plate HLAW's, alternate-side welded to give a full-penetration T-joint, were TIG-dressed.

These demonstration-of-concept TIG-dressing runs were performed manually. The two TIG-dressing conditions developed are illustrated in Figure 2.7. Both used conditions 160A arc-current and torch at right-angles to longitudinal axis (slope= 90°).

The 160A current used was the maximum capability of the welding set used; less than the recommended capacity of 250A [13, Appendix C]. Higher currents would have been tried if available. It is therefore cautioned that these results should be considered illustrative rather than a recommendation.

For the single-run single-torch TIG-dress, the torch bisected the joint angle; therefore tilt= 45° . The torch was weaved to spread melting. TIG-dressing travel speed was not measured but was slow compared to the “two runs” method. These observations suggest a considerable insufficiency of welding current for the single-run method.

For the two-runs or two-torches method, the torch was aimed at a point on the plane of the plate surface 2.5mm from the prior joint corner position.

The torch “tilt” angle is as close to geometric normal to that plate as access allowed. Thus, tilt angle was approximately 70° from the plate on which the weld toe was being dressed.

The two-pass TIG-dressing was performed at a travel speed of 0.22m/min.

Chapter 3

Results

3.1 Current-practice MIG and FCAW T-fillet welds

The FCAW fillet appearance forms Figure 3.1. The LHS image is the sample welded at 225A 23.0V. The RHS image shows a weld at slightly higher arc voltage and current of 236A and 23.5V.

The datalog for the “305/23.0” FCAW run is graphed in Figure 3.2, alongside a representative manually-welded spray-transfer MIG run for comparison. The FCAW to supplied specification looks to “short-circuit” a lot. No datalog was obtained for the explorative “320/23.5” condition. The manually manipulated MIG weld was in spray transfer at 250A 29.8V, accepting hint of “rasping sound” from arc in compressing the spray-cone. Corresponding slight short-circuiting evident in V-I plot.

3.2 Hybrid Laser-Arc Welds (HLAW’s)

Effect of changing laser-beam power is shown in Figure 3.3 where all other welding variables have been kept constant as listed in Section 2.5.3 on page 12. Each row has a laser power; from top to bottom 3.0kW, 3.5kW, 4.0kW and 4.5kW, respectively. Each row has on LHS the complete alternate-sided weldment and on RHS a single partial penetration weld at these welding conditions.

Evaluation of the outcomes is in Section 4.1.2 on page 27.

Microscopic examination provides fine-scale information on the soundness (absence of void-defects like pores and cracks), cleanliness (absence of non-metallic inclusions) and metallurgical structure. Figure 3.4 shows mi-

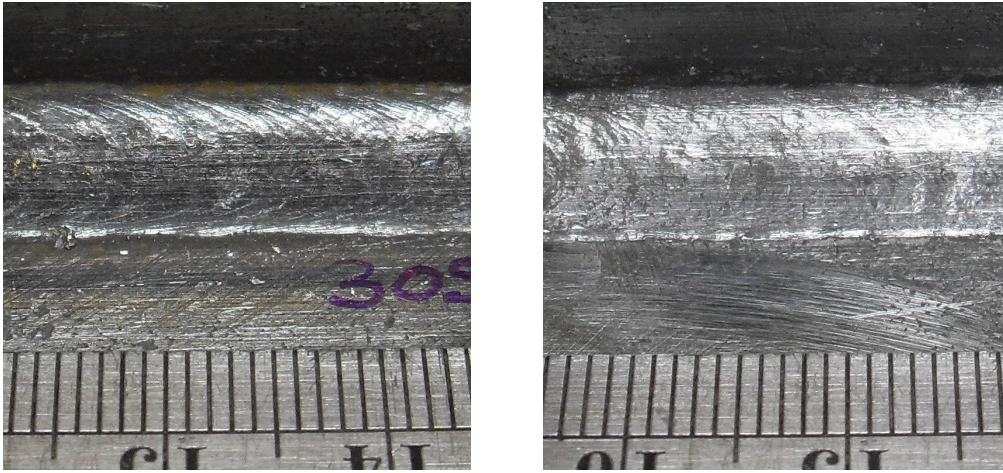


Figure 3.1: Weld surfaces of FCAW's

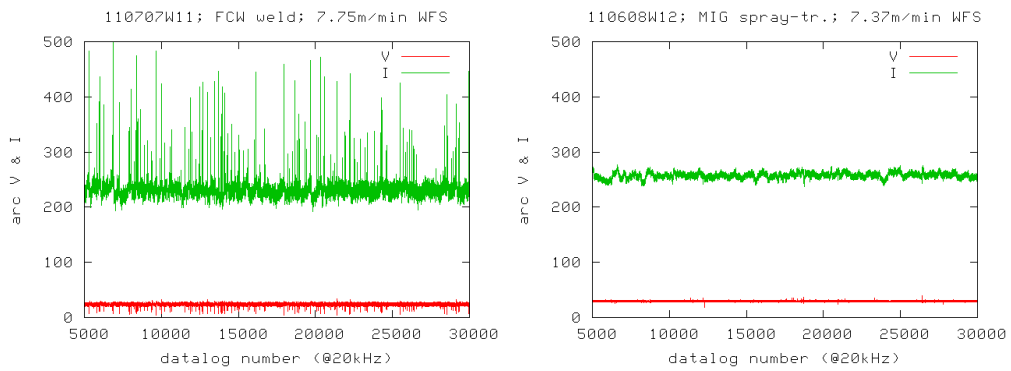


Figure 3.2: V-I plots of FCAW and GMAW datalogs

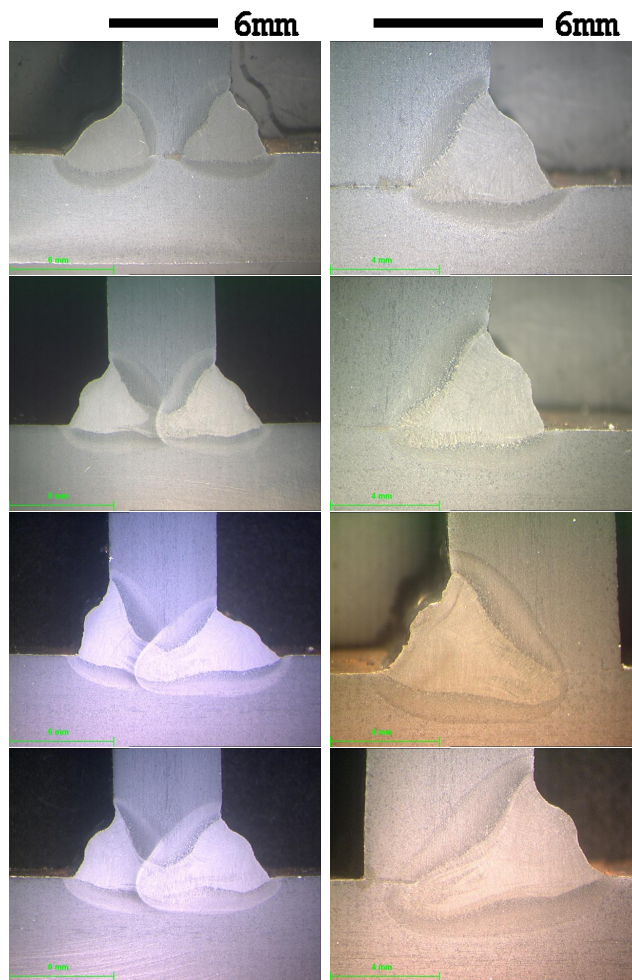


Figure 3.3: HLAW's at different laser powers - by row from top: 3.0kW, 3.5kW, 4.0kW and 4.5kW

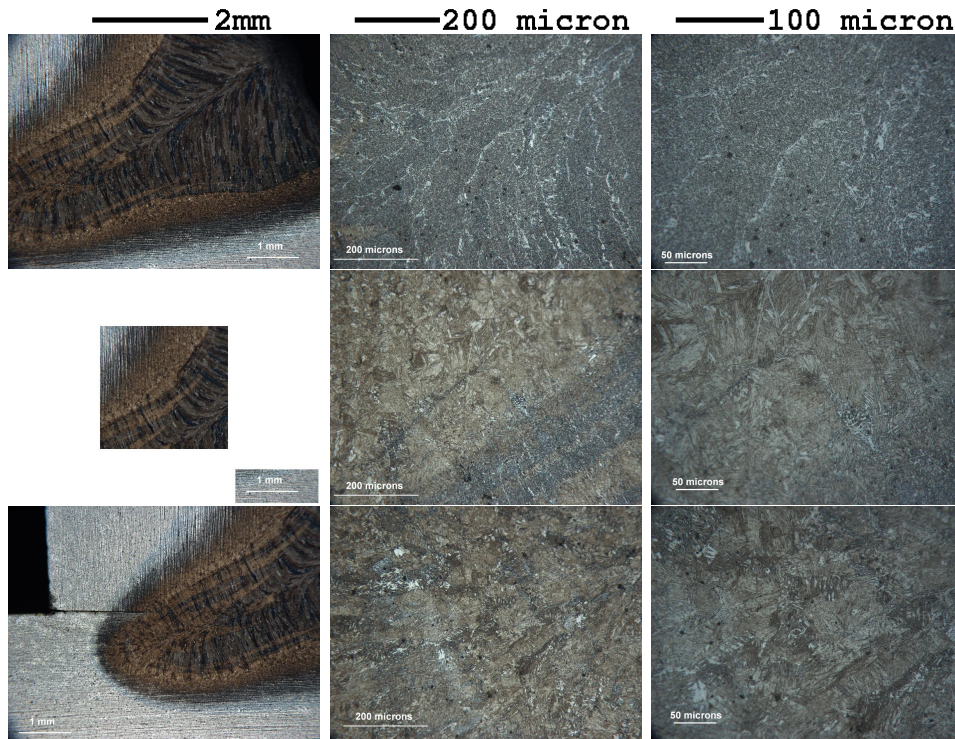


Figure 3.4: HLAW microstructures for 4.5kW - centre, HAZ and fusion-root

crostructure for a single weld using the 4.5kW laser-beam power condition. The rows present microstructure at, from top to bottom: centre of weld horizontally and vertically; HAZ of weld to terminating “T” plate at weld horizontal centre and the fusion-root. *[The microstructures are probably representative for all this family of welds: single welds and alternate-side-welded full-penetration joints; at all four laser beam powers - however time constraint prevented necessary verification]*

Metallurgical cleanness and freedom from void-type defects was inspected by viewing the polished sections not etching. Figure 3.5 shows first the etched-sample view of the same location then the as-polished view at different magnifications at the same location. The rows - top is the centre of weld horizontally and vertically; bottom is the fusion-root. The single pore near the fusion root, the largest found across the cross-section, is very small at around 20microns. It is probably causally connected to the geometric gap of the joint fit-up and is similar size to inclusions in the plate metal. It would be remelted by the alternate-side weld.

The view shows the weld has a very fine distribution of inclusions, probably finer than possessed by the plate metal. There are no crack defects and

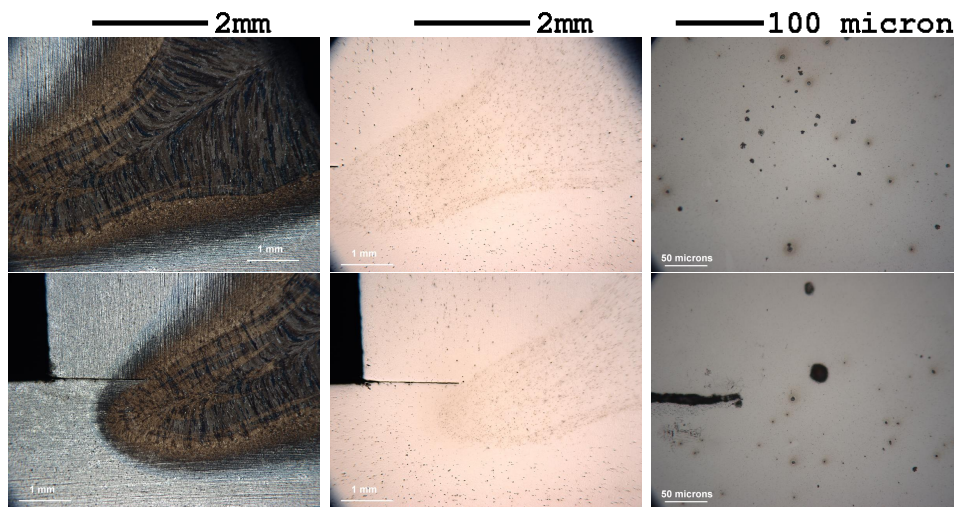


Figure 3.5: Cleanness and soundness of HLAW with 4.5kW laser beam power

very few pores, these being no larger than inclusions in the plate metal.

[hardnesses of microstructure at fusion-root and HAZ needed to indicate whether within common 350H_v max. limit and whether predominantly bainite or martensite structure]

Fatigue tests were performed on the sample welds described in the next section, 3.2.1, produced in accordance with the evaluation of this series of welds.

3.2.1 HLAW samples for fatigue testing

The weld-bead surface appearance of these welds is seen in Figure 3.6. To LHS is the HLAW with WFS=4m/min TS=1m/min and laser power=4.5kW. To RHS is the HLAW with WFS=8m/min TS=2m/min and 5.5kW laser power.

Etched “macro” cross-sections of the WFS=8m/min TS=2m/min 5.5kW laser power HLAW and a laser-only weld was made with 4.5kW of laser power at 1 m/min travel-speed are presented in Figure 3.7. The laser-only “keyhole” extension of the HLAW and the laser weld have cracks, which appear to be shrinkage cracks.

The arc power-source waveform of these HLAW’s was investigated. The waveform during a WFS=4m/min TS=1m/min laser power=4.5kW HLAW are compared to a “RapidArc” waveform with WFS=5.1m/min in conventional MIG welding in Figure 3.8.

The MIG process would not run stably on its own at these conditions

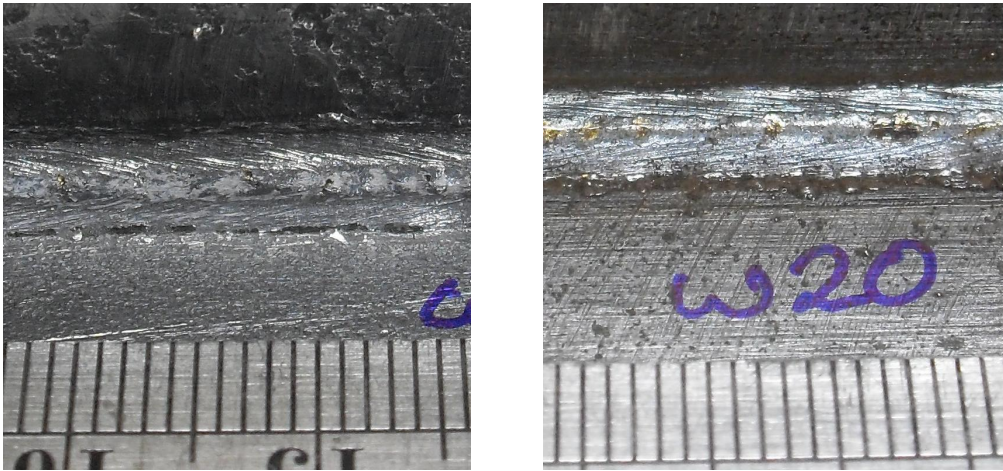


Figure 3.6: HLAW as-welded surfaces

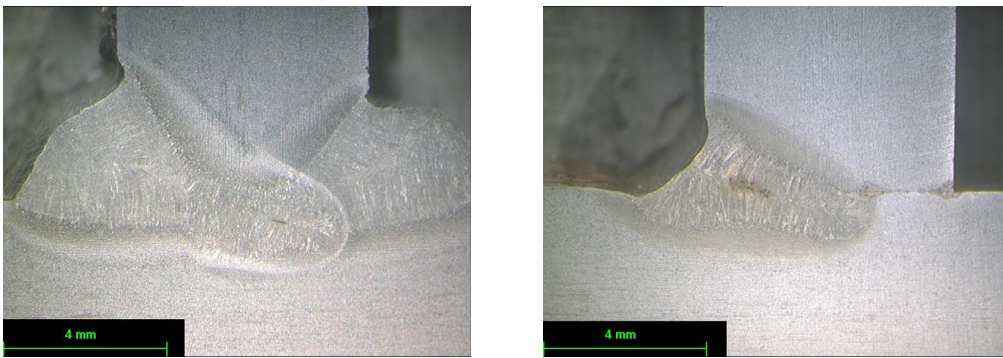


Figure 3.7: HLAW and laser weld with shrinkage cracks

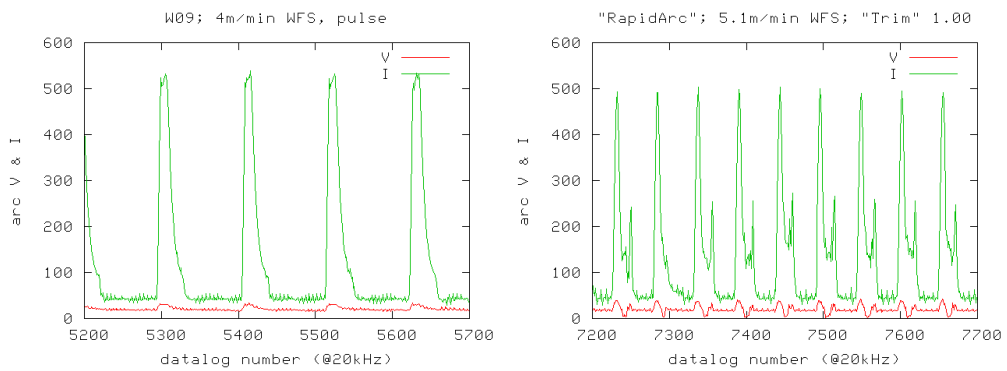


Figure 3.8: Arc waveforms: LHS - HLAW; RHS - manual "RapidArc" weld



Figure 3.9: TIG-dressed HLAW using the single-run technique

without the laser; the good welding condition seemingly being synergy between arc and laser.

3.2.2 TIG-dressing of hybrid laser/MIG welds

Photographs and photomicrographs of the cross-sections of the TIG-dressed welds are presented in Figure 3.9 for the single-run and Figure 3.10 for the two-run techniques.

The single-pass TIG-dress is appears too narrow to be confident that it will always melted-out the weld toes.

Two TIG-runs at close spacing about the centre, such that the TIG-melting overlaps, has a smooth concave radius and uniform melting reaching beyond the weld-toes by a satisfactory margin.

During the TIG-dressing activity, it was observed that weld defects, particularly those associated with the HLAW over-running a tack-weld, caused a spitting of molten metal which contaminated the tungsten of the TIG torch.

[Hardness measurement of weld fusion-root and HAZ would indicate if the TIG-dress gave relief from high hardness if that were indeed a problem for the as-welded HLAW's]

3.3 Fatigue testing of the weld samples

Fatigue testing was performed on samples of “traditional” MIG and FCAW T-fillet joints and on HLAW welds both as-welded and TIG-dressed.

3.3.1 Fatigue endurances

The fatigue endurances recorded are presented in Table 3.1.

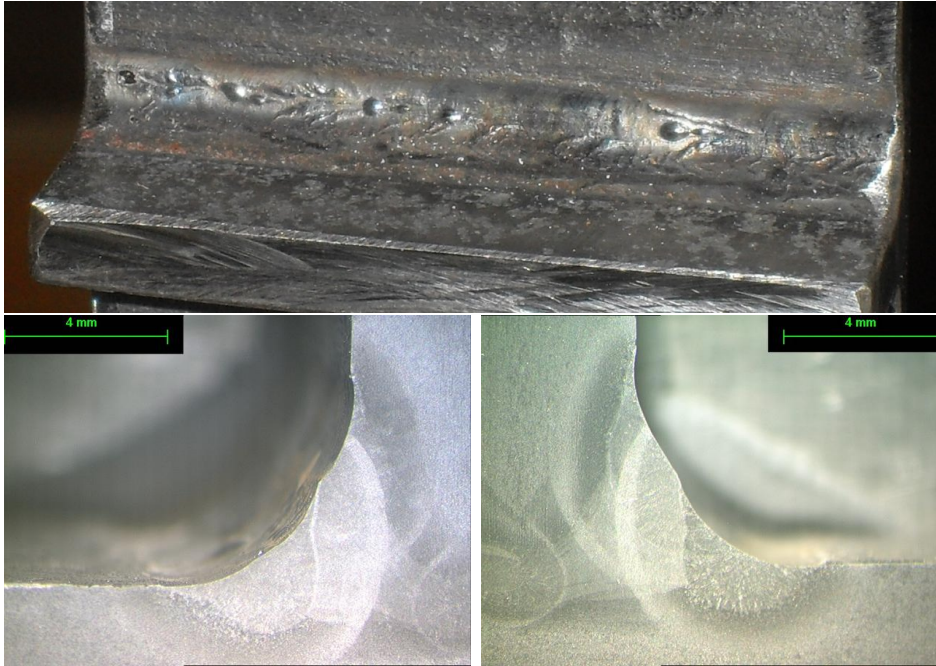


Figure 3.10: TIG-dressed HLAW using the two-run technique: overall appearance and two sections at different locations

All samples are the uniaxial pulsating-tension loaded “non-load-bearing T-joint” welds samples. BS7608:1993 does not predict fatigue endurance at stresses $>0.6\sigma_y$; hence this note where the maximum stress is higher. Where break/not-break is “no” and there is an asterisk after the N/N_{mean} ratio of observed to mean expected endurance, the test was discontinued before the sample had broken by fatigue.

These results are presented in “S-N curve” format, Figure 3.11. The lines labeled “B”, “D” and “F” are the BS7608:1993 mean-endurance lines for design-detail Classes B, D and F, respectively, against which the achieved endurance can be compared. In BS7608, for the fatigue endurance of representative commercial welds, “Class F” represents fillet welds, “Class D” represents a co-planar butt-weld of high quality and “Class B” represents the as-hot-rolled steel sections.

Fatigue endurance data of the most numerous applied test condition, the “ $0.6\sigma_y$ ” condition explained later in Section 4.3.2 on page 31, is compared to specifically the BS7608:1993 Class F mean endurance in Figure 3.12. This is a chart (not a graph). The purpose and meaning of this figure is explained as follows: the T-joints under consideration are conventionally arc welded as fillet welds, whose fatigue performance is described by BS7608:1993 weld

Sample test date y-m-d	stress range S_r MPa	max. stress S_{\max} MPa	R= 0.1 y/n	cycles tested N	break / not- break	BS7608:1993 Class F: N_{mean} $\frac{N}{N_{\text{mean}}}$
---------------------------------	---------------------------------	-------------------------------------	------------------	-------------------------	--------------------------	--

S355 conventional MIG welded :

110602	352.1	360.1	n	45971	yes	$>0.6\sigma_y$	n/a
110603	354.1	362.2	n	48330	no	$>0.6\sigma_y$	n/a *
110606	344.6	352.4	n	61301	yes	$>0.6\sigma_y$	n/a
110613	352.0	360.0	n	50996	yes	$>0.6\sigma_y$	n/a
110617	191.7	213.0	y	309718	yes	244982	1.26

DH36 conventional FCAW :

110708	98.6	109.6	y	3273797	no	1800000	1.82 *
110712	190.4	211.6	y	200077	yes	250000	0.80
110818	190.4	211.6	y	1472085	no	250000	5.89 *

DH36 hybrid Laser/MIG as-weld :

110801	190.4	211.6	y	449335	no	250000	1.80 *
110805	190.4	211.6	y	424637	yes	250000	1.70
110808	190.4	211.6	y	376326	yes	250000	1.51
110809	190.4	211.6	y	1624866	yes	250000	6.50

DH36 hybrid Laser/MIG TIG-dressed :

110727	190.4	211.6	y	1680305	no	250000	6.72 *
110729	190.4	211.6	y	2320006	no	250000	9.28 *

Table 3.1: Fatigue endurance observations for the T-joint weld samples

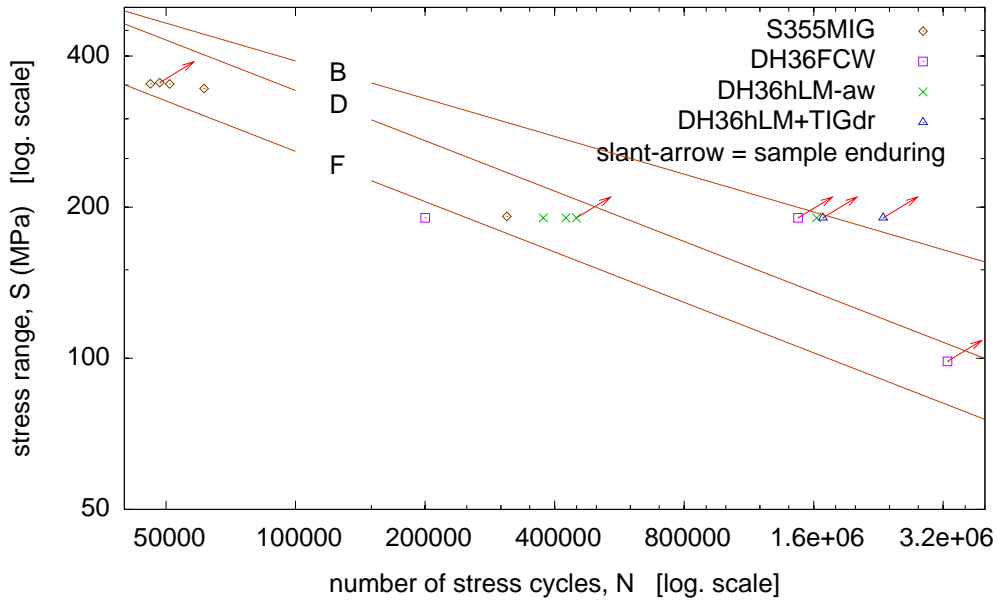


Figure 3.11: S-N curve presentation of fatigue-endurance data

detail Class F. Thus, the question anyone in the industry would ask is - how well do these welds perform compared to “Class F”? The value of the ordinate answers that question: how long the weld endured in fatigue as a multiple of the reference “Class F” endurance. As a chart, the abscissa has no physical meaning and the lines only group like data. Results above the horizontal line at “1” exceed the BS7608:1993 “Class F” performance. Results below this line are inferior to BS7608:1993 “Class F” performance.

The vertical arrows above data-points signify the sample survived unbroken at this number of cycles when the test was discontinued.

Naming: “S355” is the commercial 5mm thickness S355 plate [16]; “DH36” is the shipbuilding specification 6mm thickness plate; “MIG” is conventional MIG (only) welded; “FCW” is conventional FCAW-only; “hLM” is hybrid Laser/MIG welded; “-aw” is as-welded; “+TIGdr” is a weld which has been additionally TIG-dressed.

3.3.2 General appearance of fatigue breaks

All fatigue cracks initiated in the mid-width of the sample, away from the sample edge, at a weld toe.

Figure 3.13 shows a completed fatigue test, with the sample just broken in fatigue and its fracture-face. This is the “110602” sample of Table 3.1 on

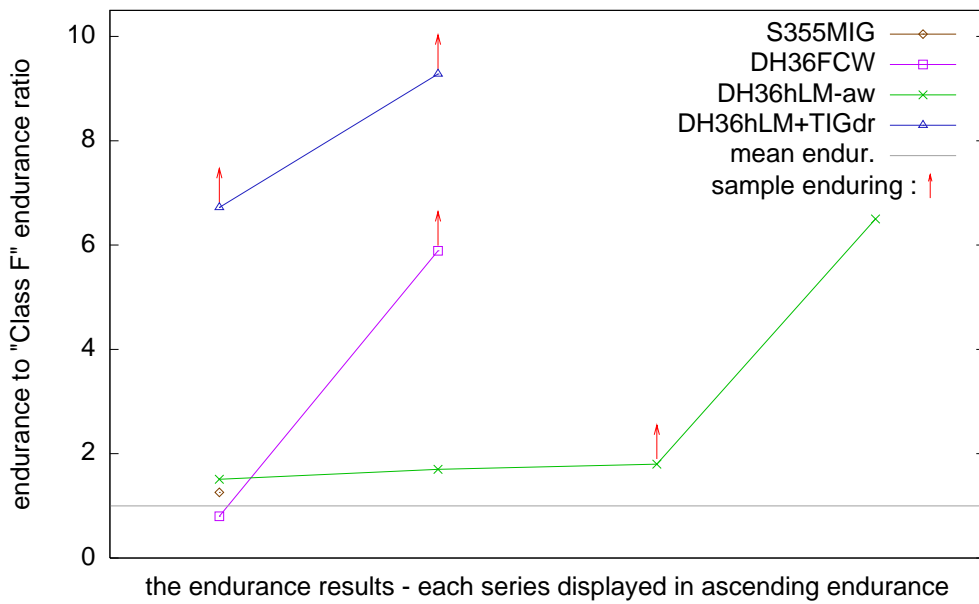


Figure 3.12: Sample endurance in ratio to the BS7608:1993 “Class F” mean endurance

page 23.

Another fatigue fracture is presented in Figure 3.14, showing an early-stage crack preserved by the final failure event from a neighbouring larger crack. This is the “110805” sample of Table 3.1.



Figure 3.13: Fractured fatigue sample

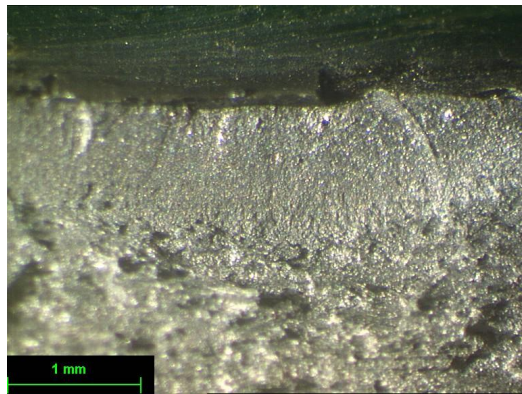


Figure 3.14: Early-stage fatigue crack, seen at top of image

Chapter 4

Discussion

4.1 The welding conditions development

4.1.1 Current-practice MIG and FCAW T-fillet welds

These welded without difficulties using welding conditions and producing welding outcomes representative of current industrial practice.

Samples were obtained using MIG dip-transfer mode, MIG spray-transfer mode and FCAW; the welding representing commercial practice.

Welding outcomes are presented in Section 3.1 on page 15.

4.1.2 Hybrid Laser-Arc Welds (HLAW's)

In Figure 3.3 on page 17 a laser power of 3.0kW is definitely insufficient, leaving a region of unfused plate in the mid-width of the joint. Laser power of 3.5kW gives overlapping penetrations but not by much margin. As repeatability is not known at present, 4.0kW appears prudent for good interlinking penetrations giving a full-penetration joint when alternate-side welded. However, uniformity and smoothness of weld-bead were better at 4.5kW of laser power, seen in Figure 3.6 on page 20, LHS image. This condition was selected for later stages of this programme. HLAW penetration looks in Figure 3.3 to be somewhat excessive for the 4.5kW weld. It is suspected that a better condition would be more arc-power while staying at 4.0kW of laser power; however with shortage of time the available usable 4.5kW condition was accepted as a matter of expediency.

For the application, the deep-penetrating characteristic, compared to a MIG / FCAW, readily provided full-penetration T-butt joints. It is fully sound, see Figs 3.4 and 3.5 on pages 18 and 19 respectively.

The special interest in this “fully-hybridised” HLAW was the speculation that it provided the start of a route to a commercially viable highly fatigue-resistant joint. It was known from literature that surface-dressing of welds can produce spectacular increases in fatigue performance [13, 15, 14, 22, 23]. TIG-dressing is visualised as integral in the following sequence:

- the “fully hybridised” HLAW provides a full-penetration T-joint, where all strength is provided in-section
- therefore, the weld beads are not required for “static strength” and serve only as “profile beads”
- the “fully hybridised” HLAW readily provides small beads on a T-joint – much smaller than a MIG/FCAW-alone weld could stably reduce to
- the small size of the “profile beads” enables a remelting process to dress the entire width of these “profile beads” in one pass along the weld joint pointing at the joint corner
- the remelt dressing means that the as-welded HLAW need not have a perfect surface quality, within reason, as small surface-form defects will be eliminated

This postulation was found to work as described, with the performance outcome suggested - results in Table 3.1 pg23, S-N plot Fig3.11 pg24 and comparative chart Fig3.12 pg25. The welds could prove to be economically viable and are discussed in Section 4.2.3.

Details on HLAW conditions

Roepke et al [8] postulate a good condition exists at a shorter axis-to-axis distance between arc and laser is less than their minimum of 4.5mm. A 2mm axis-to-axis distance is found to be optimal [9]. The axis-to-axis separation of laser and arc used here is 2mm and good welds were obtained.

Better surface and weld overall were found when the MIG arc lead the laser beam (“arc leading”). Roepke et al [8] and Campana et al [9] used laser-leading.

Change between arc-leading and laser-leading was achieved by changing the direction of traverse of the torch past the weld. As a consequence, MIG torch angle was “pushing” with laser-lead and “dragging” with arc-lead. It is therefore not known which change is important; laser lead *vs* trail or MIG “push” *vs* “drag” (or both).

This weld is “fully hybridised” in that no part is purely MIG-weld and no part is purely keyhole-laser in form; the weld tapers fairly uniformly from

widest at surface to narrowest at fusion-root; it has a depth around $1.3\times$ to $1.5\times$ the width at the surface. Roepke et al also comment on this shape.

The proprietary Lincoln “RapidArc” pulsed MIG process [24] was used for all sample joints for dressing and fatigue-testing. Effort was made to obtain good welds with the standard CV (constant voltage) operating modes – dip-transfer and spray-transfer. However, it had to be granted that on inspection, the “RapidArc” gave a much superior weld bead surface, for smoothness and regularity, than the CV modes for this application of a small fast weld Lincoln claim [24] that the process can make small weld beads at high travel-speed because it incorporates a dipping event around which control can keep a short arc. Plots of datalogs of manual-welded trial “RapidArc” welds are compatible with the claimed mode of operation. There is seen to be a large pulse, a dipping event then a smaller pulse. An example can be seen in Figure 3.8 on page 20, see RHS plot. However, absence of dipping event, operating apparently in model pulse mode, is seen for a mechanised HLAW, LHS plot of Figure 3.8.

That the “fully hybridised” partial-penetration HLAW’s are fully sound contrasts with voids and porosity of partial-penetration laser-only welds [25], caused by keyhole instability.

Laser-only “keyholes” possessed shrinkage cavities, see Figure 3.7 on page 20, not found with HLAW’s. The “2m/min travel-speed” HLAW had excessive laser power: hence the keyhole with flaw extending below the hybrid region.

4.2 Hybrid Laser/MIG weld surface remelt dressing treatments

4.2.1 The TIG dressing technique

Conditions developed for TIG-dressing are shown in Figure 2.7 on page 13. The variables seem not particularly critical and the process readily gives good results; about which others concur [13, (Appendix C)].

TIG-dressing travel speeds of 80mm/min to 160mm/min in [15] are exceeded by the two-passes technique at 220mm/min despite the 160A restriction. With more TIG current available, attaining the 1m/min TS of the developed HLAW would be an aspiration.

The rectifying action of remelt dressing when eliminating void defects causes molten metal spitting, contaminating the TIG tungsten. Plasma-dressing is reported to perform well [23, 13] and the recessed, shielded internal mechanism protects against liquid metal spatter.

4.2.2 TIG-dressing performance

The TIG-dressed HLAW's are presented in Figure 3.9 and Figure 3.10, page 22. The favoured two-run condition seen in Figure 3.10.

There is a near-perfect concave radius to the dressed profile-bead. A smooth concave radius is the general idea for a fatigue-resistant detail between two surfaces on different planes.

The width of melting adequately extends beyond the weld toes, as would make the process insensitive to moderate changes in as-welded bead shape.

The depth of melting is abundantly beyond likely as-welded toe defects without being pointlessly excessive. As a guide to good melt depth, weld toe-grinding technique description mentions ideal depth in absence of gross defects as being in the range 0.8mm to 1mm [13, (Appendix B)]. The "shallow" two-run TIG-dress melting exceeds 1.5mm, Figure 3.10 page 22, and appears ideal for purpose.

The same Figure 3.10 shows similar depth of melt in the mid-width of the dressed weld, implying that if the profile-bead were seriously undersized due to filling excessive joint set-up gap the dressed profile is likely to remain smooth.

4.2.3 TIG-dressing in a commercially viable welding option

In Section 4.1.2 starting on page 27 is listed a five-point logical progression offering a commercially viable T-joint of very highly fatigue-resisting performance. The specification inseparably couples HLAW to remelt-dressing. The high fatigue-resisting performance of these joints has already been confirmed, see results Table 3.1 on page 23, S-N plot Figure 3.11 on page 24 and comparative chart Figure 3.12 on page 25.

Regarding commercial viability, the penultimate point about the remelt-dressing activity only having to pass along the joint in unconditional relation to the joint corner location most appears to make the treatment economical. This makes the treatment feasible for a robotic process.

The visualised application is during a "factory" process; a fabrication-line in an enclosed controlled-environment location. Panels for ships are fabricated on large level tables served by gantry-robots.

The treatment has costs, of which the direct cost may be small though indirect cost like removing increased distortion may be larger. However, performance improvements suggested, Section 4.3.6, could justify these costs.

4.3 The fatigue testing programme

All fatigue tests applied a sinusoidal pulsating tensile load cycle which was invariant during a test. Apart from the first two tests, where the test frequency was being increased from lower rates with increasing experience, the test frequency was 10Hz. No effect of test frequency is expected at these low frequencies [4].

The results, in the form of the specified fatigue load-cycle, the type of weld these cycles were applied to and the endurance achieved, are all listed in Table 3.1 on page 23.

4.3.1 Use of non-load-bearing T-joint tests

The non-load-bearing (NLB) transverse T-joint samples proved appropriate for rating fatigue performance of the welds tested. Photograph and illustration of this sample configuration forms Figure 2.1 on page 7.

In all cases where the sample broke, this was in fatigue from the mid-width of the sample at one of the two weld toes. Clearly, the welds which were the object of the test were being tested.

The non-load-bearing (NLB) transverse T-joint is the fatigue test configuration used in works which have made significant contributions to fatigue knowledge; examples [13, 14].

It easy for those who have not studied fatigue to doubt the value of a test-piece where the feature being tested is not loaded in any external or obvious way. The reality could not be more different. Looking to application of welds, the converse case asserts itself. A weld is a fatigue issue whether it is load-bearing or non-load-bearing. A most severe warning is spelled out in a Welding Technology Institute of Australia (WTIA) guidance note [26] that any weld even if non-structural and for trivial purpose imposes its fatigue performance on the overall structure.

4.3.2 The 0.6 of Yield Stress fatigue test condition

The most-used fatigue test condition applied a stress-range of 190.4MPa, with an R-value of 0.1, as seen in Table 3.1 on page 23. The R-value is minimum stress / maximum stress, $\sigma_{\min}/\sigma_{\max}$, of the test stress cycle. Therefore the 190.4MPa stress-range applied itself in a load cycle between 21.2MPa minimum and 211.6MPa maximum.

The reason for these tests is applying the most severe fatigue testing condition which fits within the BS7608:1993 [11], Section 4.1 “Tensile stress limitations”. This stipulates maximum tensile stress in a fatigue condition

should not exceed 60% of the yield stress for the guidance of the code to remain valid. Regarding this investigative programme, the stipulation means if $0.6\sigma_y$ is exceeded the results may not fit on the “S-N curve”. Although called “the S-N curve” the plot of $\log S$ vs $\log N$ is linear over a very wide range of stress range S and number of cycles to failure N . This is seen in the linear plots of fatigue endurance in BS7608:1993 [11] Figures 8 & 9 and BS EN 1993-1-9:2005 [12] “Eurocode 3: Design of steel structures – Part 1-9: Fatigue” Figure 7.1 .

The steels used in this testing programme, “S355” and “DH36”, have a nominal yield stress of 355MPa. By the rule described above, the maximum stress in the fatigue test cycle must not exceed 213MPa.

An R-value of 0.1 is the closest usable repeatable condition to the desired R-value of 0 (the load cycles from zero to a chosen value). This issue is mentioned in Section 2.3.2, see page 9. An R-value of 0 caused problems for the testing machine used, as it produced mechanical “clanking” (noise and mechanical shocks sensed by touching the machine) when passing through zero load. R=0.1 keeps a small tensile stress on the sample at the lowest load of the fatigue stress cycle and is a repeatable condition which can be applied for different stress ranges.

A stress range of 191.7MPa and R-value of 0.1 makes the peak stress 213MPa - exactly $0.6\sigma_y$

A stress range of 190.4MPa and R-value of 0.1 makes the peak stress 211.6MPa. This stress range was chosen because the BS7608:1993 Class F mean endurance at this stress range is 250,000 cycles.

The $0.6\sigma_y$ condition was developed for two reasons

- at 10Hz the BS7608:1993 Class F mean endurance of 7 hours gives a convenient overnight test
- high fatigue performances obtained made high stresses the only relevant testing condition

4.3.3 Conventional MIG and FCAW cycled to the nominal yield stress

This part of the programme has the early samples forming the “learning curve” for fatigue testing and fatigue performance. MIG-welded 5mm thickness S355 plate samples were cycled between low stress and the nominal yield stress. The objective was to familiarise with the fatigue testing machine and the nature of fatigue testing.

The BS7608:1993 maximum stress of $0.6\sigma_y$ is exceeded - an issue discussed in previous Section 4.3.2. Never-the-less, the endurances measured have

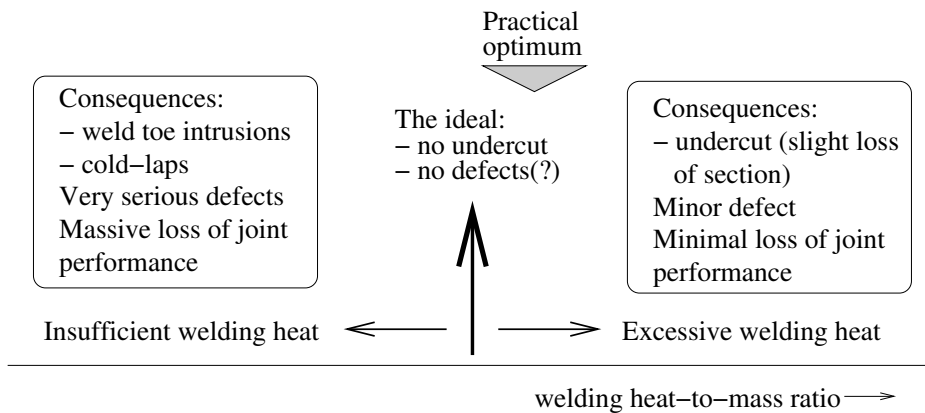


Figure 4.1: Toe-groove or “undercut”: the unequal consequences of erring about the ideal condition

interest. Endurances were $4e4$ to $6e4$. This would be good news if the application were for instance a pipeline, with very high service stress but load-cycles running into no more than a few hundred in a pipeline lifetime of some tens of years.

4.3.4 Conventional MIG and FCAW in S-N range

Limited testing machine availability meant only a few of these tests were performed.

Three results are for the $0.6\sigma_y$ condition so can be compared.

Two of the $0.6\sigma_y$ results accord with the BS7608:1993 Class F, which generally represents fillet welds, of $N_{\text{mean}}=250,000$. These are: 309718 cycles to break for the “S355” MIG-welded sample and 200077 cycles for the “DH36” FCAW to shipyard conditions sample.

The superficially identical “DH36” sample with 1472085 cycles not broken presents an interesting case. A single fatigue sample does not support extensive analysis of factors influencing fatigue performance.

This FCAW sample was welded with a higher voltage of 23.5V, compared to 23.0V suggested, when welding conditions were being explored.

Higher voltage in wire-fed welding increases fluidity of the weld-pool. The weld toes do appear more rounded at the higher welding voltage. Figure 3.1 on page 16 might enable this to be verified. [*Quantitative measurement would be appropriate*].

As a pilot study, it is suggested that the full project should test the validity of the the hypothesis advanced in Figure 4.1.

This is speculating that a fluid weld which produces a “wetted” (rounded)

weld toe avoids the sharp toe intrusions proven to cause the very low fatigue endurance of welds [10].

Welding specifications often stipulate “no undercut”. This would systematically push conditions to the conditions to the LHS of Figure 4.1 as welders comply.

It is proposed that visible undercut at the weld toe be known as “toe groove” [27]. Three categories of undercut are identified [27]. Only the almost benign “toe groove” is visible on inspection. The other two categories are the hidden weld toe intrusions with disastrous effect on fatigue performance [10].

Two pertinent questions:

- are “toe groove” and sharp toe-intrusion undercuts mutually exclusive?
- are shallow large-radius weld toe-grooves associated with good fatigue performance?

If so, welding specifications should mandate shallow large-radius toe-grooves are allowable, encouraging welding with good heat and fluidity giving “wetted” weld-toes erring towards toe-groove.

The limited effect of loss-of-section undercut (toe groove) on mechanical properties is demonstrated in empirical tests [28].

4.3.5 HLAW as-welded fatigue tests

All as-welded HLAW fatigue tests applied the “ $0.6\sigma_y$ ” test condition. This series of samples performed well, see Figure 3.12 on page 25. The lowest-performing had a fatigue endurance 1.5 times the BS7608:1993 Class F endurance, Table 3.1 on page 23.

The HLAW’s may be satisfactory as-welded and give major economic advantages compared to traditional arc-process fillet-welds. The welding speed is rapid: 1m/min provided the fully sound welds and 2m/min provided welds with excellent external surface. The shrinkage defects in the 2m/min weld sample looks to be due to an excess of laser power and may prove entirely unconnected to the welding travel speed. Weld distortion is certainly not higher than for conventional FCAW fillet welds for same service, which have arc energy of 0.62kJ/mm, results page 15. The HLAW with 4.5kW of laser power has welding energy of 0.45kW (3kW of arc energy, S2.5.3 starting pg12, with 4.5kW of laser power at 1m/min) - 73% of the FCAW energy. A direct relationship between heat input and distortion produced is observed [3], implying the HLAW’s should give lower distortion than FCAW and GMAW. “Heat input” requires knowledge of efficiency of transfer of weld energy to heat in weldment - hence weld and arc energy is quoted. As-welded

HLAW distortion needs to be accurately measured in full-length-weld trails. Lower weld distortion reduces the reputedly significant proportional cost of the entire fabrication in removing that distortion.

4.3.6 HLAW+TIG-dressed weld fatigue tests

Two welds were fatigue-tested at the $0.6\sigma_y$ condition and neither was broken by the 1680305 cycles and 2320006 cycles they respectively endured.

The fatigue test cannot be made any more severe by imposing a higher stress-range because of the $0.6\sigma_y$ maximum stress limitation, Section 4.3.2. BS7608:1993 indicates that these endurance are getting into the range of fatigue failure of as-rolled sections in perfect condition. There is the possibility that these welds are “unfatiguable” by reason of the surrounding plate being no more resistant to fatigue than these welds themselves. It would be interesting to investigate this possibility by obtaining use of a high-testing-rate resonant fatigue testing machine which can continue a test to enough cycles for some part of the sample to fatigue.

For now, what is the ultimate fatigue performance of these HLAW+TIG-dressed welds remains unknown.

Failure in plate away from the weld has been observed for TIG-dressed samples [13]. TIG-dressing is shown to perform well at all loadings of stress-range and mean “preload” stress applied and for all mixed-stress cycles [13].

The weld region of both the samples fatigue-tested was subsequently tested by magnetic-particle inspection and neither showed flaws. The implication is that there is a dominating fatigue crack initiation process bestowed on these welds. The obviously extensive crack initiation phase is far different from the general case of conventional welds [13, 26, 22, 29], where most of the much lower endurance is in resisting the crack propagation phase [13]. Creation of a fatigue crack initiation phase is noted for dressed welds [14]. The relative benefit of TIG dressing increases for higher strength steels [23].

Whether these welds would be economic, as is hoped per arguments in Section 4.1.2 on page 27, has not benefited from any further information or investigation.

Chapter 5

Conclusions

The outcome of the pilot study strongly supports proceeding to a full project on fatigue-resistant T-joints for shipbuilding and other steel structures in dynamic loading. Strong indications are that newer technologies do offer very substantially improved T-joint performance.

Hybrid laser/MIG welding followed by TIG-dressing gave the ultimate fatigue performance. Both samples tested remained unbroken and with no cracks yet formed after long tests. 2.32million cycles at a stress-range of 190.4MPa implies a fatigue resistance matching the hot-rolled steel which the weld is joining. The fatigue performance for as-welded hybrid laser/MIG welds is better than for conventional fillet welds.

Hybrid laser/MIG welds enable full-penetration T-butt joints of excellent quality where there is both-sides access to the joint. A good operating condition appears to balance arc energy and laser energy giving a weld about 1.3 times to 1.5 times as deep as it is wide at the surface, uniformly tapering to narrower fusion-root. This weld has no features which are purely keyhole-laser nor purely MIG in character. These welds have no internal defects (porosity, shrinkage cracks, *etc*) and good surface form (profile good and no surface defects).

As-welded hybrid laser/MIG welds offer additional advantages over conventional arc fillet T-joints of more rapid welding speed (at least double) and may give lower weld distortion.

Single-side T-joint access invites deeply though not fully-penetrated hybrid laser/MIG welds likely to out-perform single-sided fillet welds.

Remelt dressing was simple to apply, suggesting a commercially viable weld specification combining hybrid laser/MIG with remelt dressing. TIG dressing naturally formed a smooth concave semi-circular reformed weld profile while melting-out the weld toes to desired depth. These features explain the high fatigue endurance of these welds.

Suggestions for further work

Possible future investigations:

- measure the hardness of the heat-affect-zone and fusion root of the HLAW's
- whether conventional arc welds run with a higher heat-to-mass ratio producing shallow smooth wide-radiused undercut (to-groove) give better fatigue performance.
- develop TIG-dressing to work at higher travel speeds - try to match travel speed of a HLAW
- try plasma dressing of welds seek faster, better dressing and resistance to contamination from spitting molten metal
- where only single-sided access is possible, such as for the boom of an excavator fabricated as a closed box-section, what is the deepest penetration achievable? Is it possible to fully penetrate the thickness leaving a satisfactory penetration-bead; 'just penetrated'?
- how tolerant are the HLAW processes developed to joint fit-up gap?
- extend fatigue testing programme to high-strength steels, given very high fatigue resistances attained

Bibliography

- [1] J. Norrish. *Advanced Welding Processes*. IOP Publishing Ltd, Bristol UK, 1992.
- [2] J. J. Lowke. Physical basis for the transition from globular to spray modes in gas metal arc welding. *Journal of Physics D: Applied Physics*, 42(13), 2009.
- [3] P. Colegrove, C. Ikeagu, A. Thistlethwaite, S. Williams, T. Nagy, W. Suder, A. Steuwer, and T. Pirling. Welding process impact on residual stress and distortion. *Science and Technology of Welding and Joining*, 14(8):717–725, 2009.
- [4] T. R. Gurney. *Fatigue of Welded Structures - 2nd edn*. Cambridge.U.P., Cambridge UK, 1979.
- [5] S. J. Maddox. *Fatigue Strength of Welded Structures - 2nd edn*. Abington, Cambridge UK, 1991.
- [6] W. Suder, S. Ganguly, S. Williams, A. M. Paradowska, and P. Colegrove. Comparison of joining efficiency and residual stresses in laser and laser hybrid welding. *Science and Technology of Welding and Joining*, 16(3):244–248, 2011.
- [7] C. H. J. Gerritsen. Hybrid nd:yag laser mag welding of t joints in c-mn steels for shipbuilding applications. Members report 796/2004, TWI, March 2004.
- [8] C. Roepke, S. Liu, S. Kelly, and R. Martukanitz. Hybrid laser arc welding process evaluation on DH36 and EH36 steel. *Welding Journal*, 89(7):140s–150s, 2010.
- [9] G. Campana, A. Fortunato, A. Ascari, G. Tani, and L. Tomesani. The influence of arc transfer mode in hybrid laser-mig welding. *Journal of Materials Processing Technology*, 191(1-3):111–113, 2007.

- [10] E. G. Signes, R. G. Baker, J. D. Harrison, and F. M. Burdekin. Factors affecting the fatigue strength of welded high strength steels. *British Welding Journal*, 14(3):108–116, 1967.
- [11] British Standards Institute. Code of practice for fatigue design and assessment of steel structures. National Standard BS 7608:1993, British Standards Institute, London UK, 1993.
- [12] British Standards Institute. Eurocode 3. design of steel structures – part 1-9: Fatigue. European Standard BS EN 1993-1-9:2005, British Standards Institute, London UK, 2005.
- [13] S Manteghi. Methods of fatigue life improvement for welded joints in medium and high strength steels. Members report 637/1998, TWI, March 1998.
- [14] Y-H. Zhang and S. J. Maddox. Fatigue life prediction for toe ground welded joints. *International Journal of Fatigue*, 31(7):1124–1136, 2009.
- [15] P. J. Haagensen and S. J. Maddox. IIW recommendations on post weld improvement of steel and aluminium structures. IIW Recommendations XIII-1815-00, International Institute of Welding, August 2006.
- [16] British Standards Institute. Hot rolled products of structural steels. technical delivery conditions (parts 1 to 6). European Standard BS EN 10025-1-6:2004, British Standards Institute, London UK, 2004.
- [17] British Standards Institute. Welding consumables. wire electrodes and deposits for gas shielded metal arc welding of non alloy and fine grain steels. classification. National Standard BS EN ISO 14341, British Standards Institute, London, UK, 2008.
- [18] British Standards Institute. Welding consumables. gases and gas mixtures for fusion welding and allied processes. National Standard BS EN ISO 14175, British Standards Institute, London, UK, 2008.
- [19] American Bureau of Shipping. Rules for building and classing steel vessel rules (2011) - part 2. Classification society standard, American Bureau of Shipping, Houston, TX 77060 USA, 2011.
- [20] British Standards Institute. Welding consumables. tubular cored electrodes for gas shielded and non-gas shielded metal arc welding of non-alloy and fine grain steels. classification. National Standard BS EN ISO 17632, British Standards Institute, London, UK, 2008.

- [21] J. C. Ion. *Laser processing of engineering materials : principles, procedure and industrial application*. Elsevier, Oxford UK, 2005.
- [22] L. L. Martinez. Fatigue life extension procedure for offshore structures by ultrasonic peening. In *Proceedings of the Annual Offshore Technology Conference*, volume 1, pages 104–111, 2010.
- [23] A. L. Ramalho, J. A. M. Ferreira, and C. A. G. M. Branco. Fatigue behaviour of T welded joints rehabilitated by tungsten inert gas and plasma dressing. *Materials and Design*, 2011. Article in Press.
- [24] The Lincoln Electric Company, Cleveland OH USA. *RapidArc – High Speed GMAW Welding*, (undated - obtained 2011). file *nx280.pdf*.
- [25] J. Y. Lee, S. H. Ko, D. F. Farson, and C. D. Yoo. Mechanism of keyhole formation and stability in stationary laser welding. *Journal of Physics D: Applied Physics*, 35(13):1570–1576, 2002.
- [26] WTIA. Introduction to fatigue of welded steel structures and post-weld improvement techniques. Guidance note TGN-D-02 Rev: 0, Welding Technology Institute of Australia, March 2006.
- [27] J. E. M. Jubb. Undercut or toe groove - the cinderella defect. *Metal Construction*, 13(2):94–98, 1981.
- [28] O. W. Blodgett. *Design of Welded Structures*. J F Lincoln foundation, Cleveland OH USA, 1966.
- [29] P. J. Tubby, E. J. Olden, and G S Booth. Fatigue test results for laser welds in steel - a review. Technical report 687/1999, TWI, September 1999.